Detecting Features in Spaceborne Backscatter Lidar Data: Spatial Averaging vs. Machine Learning Based Denoising

John E. Yorks[(a)], Patrick Selmer[(b)], Amanda Cresanti[(c)], Kenneth Christian[(d)], Natalie Midzak[(a)], Ed Nowottnick[(a)]

(a) NASA Godard Space Flight Center, Greenbelt, MD, USA
(b) Science, Systems, and Applications, Inc., Lanham, MD, USA
(c) Department of Atmospheric and Oceanic Sciences, Univ. of Maryland, College Park, MD, USA
(d) Earth System Science Interdisciplinary Center, Univ. of Maryland, College Park, MD, USA
Lead Author e-mail address: John.E.Yorks @nasa.gov

Abstract: Space-based lidar systems provide critical information about the vertical distributions of clouds and aerosols that greatly improve our understanding of the climate system. However, daytime spaceborne lidar signals are degraded by solar background. To overcome this issue, data is averaged during science processing at the expense of spatial resolution. New machine learning tools for denoising daytime spaceborne lidar data enable improvements in signal-to-noise ratio and data products at finer resolutions. Here we use airborne data and spaceborne simulations of backscatter lidar systems to quantify the performance of cloud detection frequencies and cloud top heights using spatial averaging and DDUNet autoencoder denoising.

1. Introduction

Vertical profiles of aerosols and clouds from spaceborne lidar are critical measurements toward better understanding the Earth's climate, weather, and air quality. Backscatter lidar systems that employ photon counting detectors are highly sensitive and enable the detection of optically thin aerosols and clouds, especially at night. Examples of such lidars include the Cloud Aerosol Transport System (CATS) that operated on the International Space Station from February 2015 to October 2017 and the Advanced Topographic Laser Altimeter System (ATLAS) that currently flies on the ICESat-2 mission and launched in September of 2018 [1,2]. Signal-to-noise ratio (SNR) is significantly lower during daytime than at night for CATS and ATLAS, limiting the ability to detect faint atmospheric features.

Daytime signals from backscatter lidars are degraded by noise from solar background light [3,4]. There are two primary ways to improve the daytime SNR of a lidar instrument: (1) increase the power-aperture factor during design and/or (2) average the data onboard or during science data processing. The power-aperture factor is limited by the volume, mass, and power constraints of the spacecraft bus. Moreover, the aerospace industry's expanding use of SmallSat buses is incompatible with simply increasing the power-aperture product to obtain better SNR. Vertical and horizontal averaging is typically utilized to improve daytime SNR and accuracy of data products, but at the expense of resolution. For example, CATS data was averaged to 60 km during daytime to detect aerosol layers [5].

Lolli (2023) provides a survey of machine learning techniques applied to lidar observations for the detection of aerosol and cloud optical, geometrical, and microphysical properties [6]. Recent work has demonstrated success in boosting SNR without decreasing resolution using advanced filtering techniques such as Wavelet denoising and Convolutional Neural Networks (CNN) for finer resolution layer detection [5]. However, rapid advancements in Deep Learning based image denoising algorithms [7,8] can further improve the SNR. Here, we will simulate the CATS daytime signal and reduce the noise by applying a Deep Learning based image denoising algorithm to quantify the improvements in aerosol and cloud detection frequencies and cloud top heights.

2. Method

Airborne Cloud Physics Lidar (CPL) [9] data from 6 field campaign cases (Table 1) and the NASA GSFC lidar simulation model [10] are used to compute synthetic data with various

© The Authors, published by EDP Sciences. This is an open access article distributed under the terms of the Creative Commons Attribution License 4.0 (https://creativecommons.org/licenses/by/4.0/).

atmospheric feature types and scenes (dust plume, smoke layer, transparent and opaque ice clouds, mid-level mixed phase clouds, stratus clouds). The airborne CPL data was used to provide the atmospheric backscatter and extinction terms in the lidar equation and are considered the "Truth". These features/scenes are simulated using the CATS instrument parameters [11] for daytime conditions with solar background noise computed over land with a solar zenith angle of 30 degrees.

Table 1. CPL Cases for Simulations

Project	Date	Feature Types
IMPACTS	01/05/23	Ice clouds
	02/13/22	Mixed cloud types
	02/23/20	Ice clouds, cumulus
ICESat-2 Validation	10/28/19	Smoke
CATS Validation	8/18/15	Smoke, transparent cirrus
HS3	8/21/13	Dust Plume

The daytime simulated CATS data will be processed using the standard CATS operational algorithms [5] to create the 60 km average dataset. A state-of-the-art Deep Learning image denoising algorithm is then applied to the daytime simulated CATS lidar curtain images for all 6 cases to create a 2 km denoised dataset. Specifically, a DDUNet neural network model [8] architecture was trained using CATS raw 1064 nm photon count data. Artificial Poisson noise was added to night CATS data to create the noisy and noise-free image pairs. The training dataset was created using these pairs of noisy (daytime simulations) and noise-free (actual nighttime data) CATS lidar curtain images. We then used these images to train the DDUNet model to predict residual noise instead of the noise-free image [8]. The latent noise-free image can then be obtained by subtracting output (noise) from input (noisy simulated data). Preliminary results on selected CATS cases show a factor of 2 improvement in SNR and attenuated total backscatter (ATB) accuracy compared to the current operational CATS data that uses averaging to overcome poor SNR. Figure 1 shows the simulated 1064 nm ATB for the 05 January 2023 case without noise (top panel), with noise (middle 2 panels), and with the DDUNet Deep Learning autoencoder denoising technique applied to the data (bottom panel).

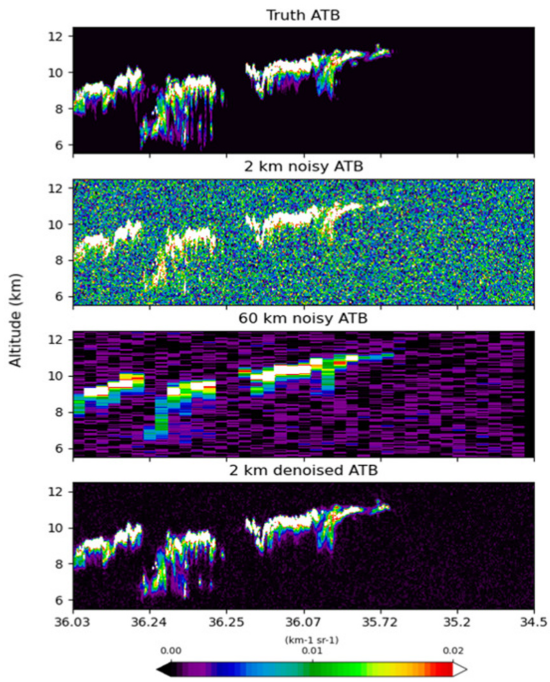

Figure 1. The 1064 nm ATB for the 05 January 2023 case for the simulated truth without noise (top panel), with noise averaged to 2 km (top-middle), with noise averaged to 60 km (bottom middle) and after the DDUNet Deep Learning autoencoder denoising technique was applied to the data (bottom panel).

3. Results

A simple scattering ratio threshold profile technique is applied to the averaged or denoised attenuated backscatter data, similar to the method used for CALIOP and CATS [5,12]. For the extended abstract, we only show results from the 05 January 2023 IMPACTS case, but will show other cases in the presentation. Figure 2 shows the bins where a layer was detected for the 2 km averaged data (top), 60 km averaged data (middle), and 2 km denoised data (bottom) compared to the truth from the simulation input for the 05 January 2023 case shown in Figure 1. The True Positive (TP, purple) show the agreement with the truth, while the False Positive (FP, red) show bins defined as a layer that were not in the truth dataset, and the False Negative (FN, teal) shows bins that are in clouds in the truth dataset but not detected in the averaged or denoised dataset. Figure 3 shows a vertical profile of cloud detection frequencies for the 05 January 2023 case for the 2 km truth dataset (black), 2 km denoised (green), 2 km averaged (blue), and 60 km averaged (red).

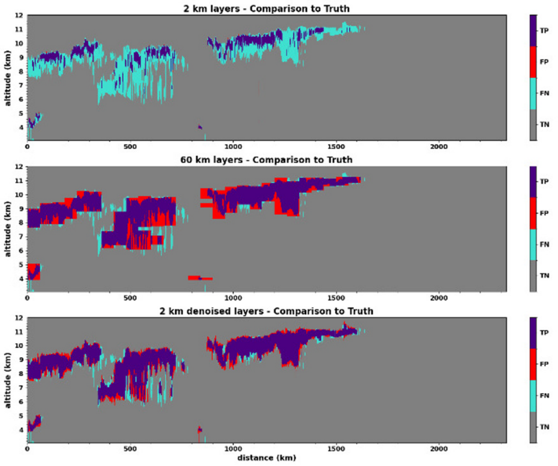

Figure 2. A vertical feature mask that shows the bins where a layer was detected compared to the truth for the 05 January 2023 case shown in Figure 1.

The DDUNet denoised data enables the best performance of cloud detection using the threshold profile technique while limiting false positive detections near cloud edges. The threshold profile technique applied to the 2 km noisy daytime simulation only detects clouds in 27% of the truth cloud bins (purple, Figure 2, top panel). It especially misses bins with weaker attenuated backscatter values and bins beyond 1 km from cloud top (teal, Figure 2, top panel) Figure 3 shows detection frequencies that are 60-70% lower than the truth dataset. This is not surprising and consistent with actual spaceborne lidar data, which is why operational algorithms for CALIOP and CATS averaged data as much as 80 and 60 km, respectively, to improve layer detection performance. Averaging the simulated dataset to 60 km and applying the threshold profile technique improves the cloud detection frequencies to 87% compared to the truth dataset (purple, Figure 2, middle panel and Figure 3, red), but now overestimates the cloud detection frequencies by about 10% compared to the truth (black). This is a result of the averaging "smearing" clouds, which extends the cloud boundaries out to bins that were not part of the cloud in the truth dataset, demonstrated by the red colors in Figure 2 (middle panel). This adds 6,127 false positives bins to the scene, nearly 3x more bins (2,267) than the false negative bins (bins not detected). The DDUNet denoised cloud detections are also 87% compared to the truth dataset, but the finer resolution limits the false positives due to the cloud smearing effect to just 3,116 bins and provides a much better match to the true cloud detection frequencies shown in Figure 3. The 87% cloud detection frequencies using 2 km DDUNet denoised data is better than the reported performance of CALIOP cloud detections, which only detected 68% of CPL "in-cloud" bins at resolutions of 5-80 km [13].

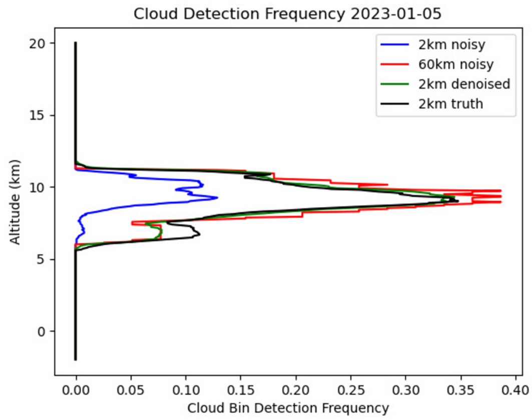

Figure 3. A vertical profile of cloud detection frequencies for the 05 January 2023 case.

Cloud top heights (CTH) detected using the DDUNet denoised data are better correlated with the CTHs in the truth dataset, with lower mean absolute error (MAE) and root-mean squared error (RMSE). Figure 4 shows histograms of the CTH difference compared to the truth for all cloud layers detected in Figure 2 for the 2 km noisy (top), 60 km averaged (middle), and the 2 km DDUNet denoised (bottom) datasets. The 2 km noisy CTHs have a low bias of about 200 m, with a RMSE of 418 m. While averaging to 60 km improves this bias, with a mean difference of +40 m, the RMSE is still close to 400 m due to the smearing effects in Figure 2. The CTHs retrieved using the denoised data at 2 km provides the best mean difference (6 m), MAE (155 m), and RMSE (344 m). This is better performance than reported by Thorsen et al. (2011) for CALIOP ice cloud CTHs compared to three ARM sites, which ranged from 350-910 m [14]. The 2 km DDUNet denoised dataset also has the most points (732) and the best correlation (0.93) based on scatter plots for all three datasets (not shown).

4. Discussion

The DDUNet Deep Learning autoencoder denoising technique described here improve the data products from photon counting spaceborne lidar systems such as CATS and ATLAS and allow us to assess the errors in standard data products due to coarse spatial averaging. A summary of the results will be added here. Tools developed for noise reduction of daytime lidar signals also enable future SmallSat lidar concept/constellation designs that can meet the volume, mass, and power constraints of the small spacecraft buses. There are currently no atmospheric lidar instruments now operating on orbit or planned for CubeSats and SmallSats. Denoising tools can produce data products from SmallSat lidars with similar or better accuracies and spatial resolutions as larger sensors, with improved spatiotemporal coverage since multiple copies would be more affordable.

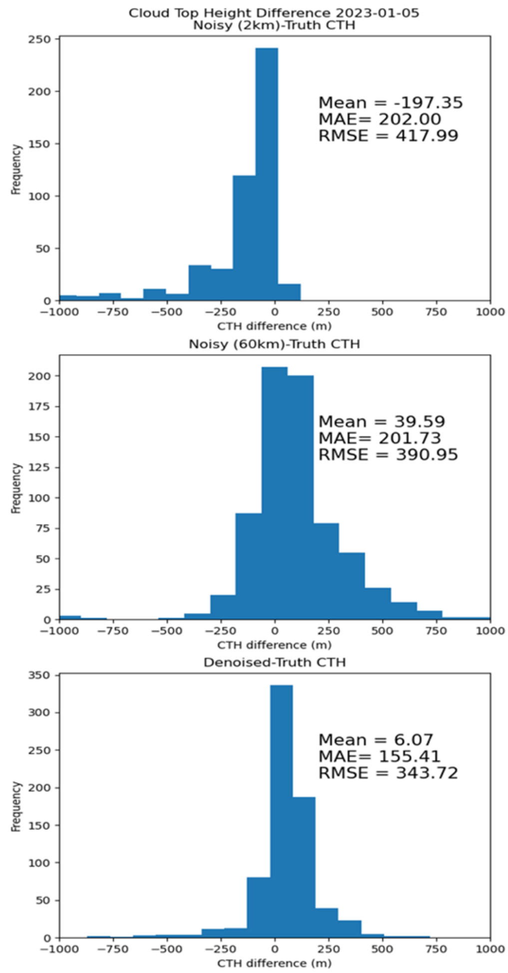

Figure 4. CTH differences compared to the truth for the 05 January 2023 case.

5. References

[1] Yorks, J. E., et al. (2016), An Overview of the CATS Level 1 Data Products and Processing Algorithms, Geophys. Res. Let., 43, doi:10.1002/2016GL068006.

[2] Palm, S. P., et al. (2021). ICESat-2 atmospheric channel description, data processing and first results. Earth and Space Science, 8, e2020EA001470.

[3] McGill, M. J., et al. (2007), Airborne validation of spatial properties measured by the CALIPSO lidar, J. Geophys. Res., 112, D20201, doi:10.1029/2007JD008768.

[4] Hunt, W. H., et al. (2009), CALIPSO Lidar Description and Performance Assessment. J. Atmos. Oceanic Technol., 26, 1214–1228.

[5] Yorks, J.E., et al. (2021), Aerosol and Cloud Detection Using Machine Learning Algorithms and Space-Based Lidar Data. Atmosphere 2021, 12, 606. https://doi.org/10.3390/atmos12050606.

[6] Lolli, S. Machine Learning Techniques for Vertical Lidar-Based Detection, Characterization, and Classification of Aerosols and Clouds: A Comprehensive Survey. Remote Sens. 2023, 15, 4318. https://doi.org/10.3390/rs15174318.

[7] Zhang, K. et al. (2017), Beyond a Gaussian denoiser: Residual learning of deep CNN for image denoising. IEEE Transactions on Image Processing, 26(7):3142–3155.

[8] Jia, F., et al. (2021), DDUNet: Dense Dense U-Net with Applications in Image Denoising. 2021 IEEE/CVF International Conference on Computer Vision Workshops (ICCVW), Montreal, BC, Canada, pp. 354-364, doi:10.1109/ICCVW54120.2021.00044.

[9] McGill, M.J., et al. (2002), Cloud Physics Lidar: instrument description and initial measurement results, Applied Optics, 41, 3725-3734.

[10] Nowottnick, E.P., et al. (2022), A Simulation Capability Developed for NASA GSFC's Spaceborne Backscatter Lidars, Proceedings of the 30th International Laser Radar Conference, Springer, https://doi.org/10.1007/978-3-031-37818-8.

[11] McGill, M.J., et al. (2015), The Cloud-Aerosol Transport System (CATS): a technology demonstration on the International Space Station, Proc. SPIE 9612, Lidar Remote Sensing for Environmental Monitoring XV, 96120A, doi:10.1117/12.2190841.

[12] Vaughan, M., et al. (2009), Fully automated detection of cloud and aerosol layers in the CALIPSO lidar measurements, J. Atmos. Oceanic Technol., 26, 2034–2050.

[13] Yorks, J. E., et al. (2011), Airborne validation of cirrus cloud properties derived from CALIPSO lidar measurements: Spatial properties, J. Geophys. Res., 116, D19207, doi:10.1029/2011JD015942.

[14] Thorsen, T. J., et al. (2011), Comparison of the CALIPSO satellite and ground-based observations of cirrus clouds at the ARM TWP sites, J. Geophys. Res., 116, D21203 doi:10.1029/2011JD015970.